

CrystEngComm

Accepted Manuscript



This is an *Accepted Manuscript*, which has been through the Royal Society of Chemistry peer review process and has been accepted for publication.

Accepted Manuscripts are published online shortly after acceptance, before technical editing, formatting and proof reading. Using this free service, authors can make their results available to the community, in citable form, before we publish the edited article. We will replace this *Accepted Manuscript* with the edited and formatted *Advance Article* as soon as it is available.

You can find more information about *Accepted Manuscripts* in the [Information for Authors](#).

Please note that technical editing may introduce minor changes to the text and/or graphics, which may alter content. The journal's standard [Terms & Conditions](#) and the [Ethical guidelines](#) still apply. In no event shall the Royal Society of Chemistry be held responsible for any errors or omissions in this *Accepted Manuscript* or any consequences arising from the use of any information it contains.



Structural, morphological and optical investigation of β - Ag_2MoO_4 microcrystals obtained with different polar solvents

Received 18th August 2015,
Revised 09th September 2015,
Accepted 00th xxxxx 20xx

F.S. Cunha^a, J.C. Szcancoski^b, I.C. Nogueira^c, V.G. de Oliveira^a, S.M.C. Lustosa^a, E. Longo^b, L.S. Cavalcante^{a*}

DOI: 10.1039/x0xx00000x

www.rsc.org/chemcomm

This communication reports on the formation of beta silver molybdate (β - Ag_2MoO_4) microcrystals synthesized by a simple precipitation method using different polar solvents [water, methanol, ethanol, 1-propanol and 1-butanol]. These crystals were structurally characterized by means of X-ray diffraction (XRD) and Rietveld refinements. The crystal shapes and sizes were observed by field emission scanning electron microscopy (FE-SEM). Their optical properties were analyzed by ultraviolet–visible (UV–vis) absorption spectroscopy. XRD patterns and Rietveld refinement data indicated all crystals have spinel-type cubic structure. FE-SEM images revealed the crystals tend to increase in average size with the reduction in the degree of polarity of the solvent. Finally, β - Ag_2MoO_4 microcrystals exhibited a dependence of optical band gap energies (from 3.30 to 3.38 eV) with the intermediary energy levels.

Silver molybdate (Ag_2MoO_4) presents two types of electronic structure, depending on the pressure conditions in which the crystal is subjected.¹ At room temperature, Ag_2MoO_4 exhibits a spinel-type cubic structure related to beta (β - Ag_2MoO_4) phase, which is more stable in nature. However, when exposed to high hydrostatic pressure, these crystals have a tetragonal structure associated to alpha (α - Ag_2MoO_4) metastable phase.² Recently, the literature³ has reported the formation of α - Ag_2MoO_4 metastable phase by the solution-phase precipitation method under environment condition, and using 3-bis(2-pyridyl)pyrazine (dpp) as doping.³ The influence of pH at starting solution on the growth and formation processes of distinct heterostructures (brooms, flowers and rods) was investigated by Singh et al.⁴ and Fodjo et al.⁵, in which the sodium borohydride was employed to induce the reduction of silver nanoparticles on the surface of Ag_2MoO_4 crystals in order to enhance the Raman scattering. In other studies, Ag- Ag_2MoO_4 composites prepared by microwave-assisted hydrothermal

synthesis presented interesting photocatalytic activity for the degradation of Rhodamine B under visible light.⁶ In addition, Ag_2MoO_4 mixed with graphite acts as a good lubricant for Ni-based composites, improving the tribological properties of this system.⁷

Different synthesis methods have been employed to obtain pure β - Ag_2MoO_4 crystals, including solid-state reaction or oxide mixture at high temperature,⁸ melt-quenching⁹ and Czochralski growth.¹⁰ Particularly, high temperatures, long processing times, and/or sophisticated equipment are necessary in these synthetic routes. Moreover, the final products may be composed of irregular particle shapes with nonhomogeneous size distribution as well as contain the presence of secondary phases. In recent years, pure β - Ag_2MoO_4 crystals have been synthesized by the co-precipitation,¹¹ microwave-assisted hydrothermal synthesis,^{11,12} dynamic template route using polymerization of the acrylamide assisted templates¹³ and impregnation/calcination method.¹⁴ Due to the peculiarity of each synthetic route with their experimental conditions, β - Ag_2MoO_4 crystals are able to exhibit different physicochemical properties as photoluminescence, photocatalysis, antibacterial action against the DH 5 α bacteria and catalytic oxidation of elemental mercury, respectively.

However, little attention has been given in the literature on the formation of β - Ag_2MoO_4 crystals using different chemical solvents in the reaction medium. Therefore, in this communication, β - Ag_2MoO_4 microcrystals were synthesized by the precipitation method, employing several polar solvents: deionized water (H_2O), methanol (CH_3OH), ethanol ($\text{C}_2\text{H}_5\text{OH}$), 1-propanol ($\text{C}_3\text{H}_7\text{OH}$) and 1-butanol ($\text{C}_4\text{H}_9\text{OH}$) at 60°C for 8 h. X-ray diffraction (XRD), Rietveld refinements and field emission scanning electron microscopy (FE-SEM) were employed in structural and morphological characterizations. The optical properties were investigated by ultraviolet–visible diffuse reflectance spectroscopy with evaluation of optical band gap values.

The experimental procedure and characterizations of β - Ag_2MoO_4 microcrystals are described in Supplementary Information.

Fig. 1(a–e) illustrates the XRD patterns of β - Ag_2MoO_4 microcrystals prepared at 60°C for 8 h with different polar solvents.

^aPPQG-DQ-CCN-Universidade Estadual do Piauí, Rua-João Cabral, CP-2231, 64002-150, Teresina-PI, Brazil (*laeciosc@bol.com.br)

^bUniversidade Estadual Paulista, CP 355, 14801-907, Araraquara-SP, Brazil

^cInstituto Federal do Maranhão, PPG em Engenharia de Materiais, 65030-005, São Luís, MA, Brazil

† Electronic supplementary information (ESI) available

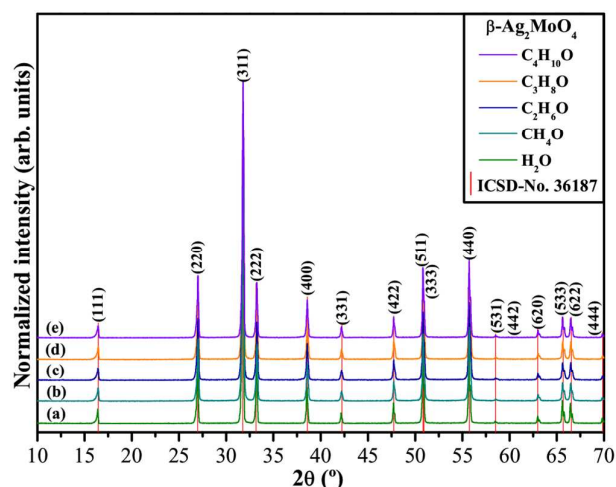


Fig. 1: XRD patterns of β - Ag_2MoO_4 microcrystals prepared with (a) H_2O , (b) CH_4O , (c) $\text{C}_2\text{H}_6\text{O}$, (d) $\text{C}_3\text{H}_8\text{O}$, and (e) $\text{C}_4\text{H}_{10}\text{O}$.

In Fig. 1(a–e), XRD patterns confirmed all β - Ag_2MoO_4 crystals have a spinel-type cubic structure, without any deleterious phase, with space group ($Fd\bar{3}m$) and point-group symmetry (O_h^7), in good agreement with ICSD card No.36187¹⁵, and literature.¹⁶ The sharp and intense diffraction peaks are typical features of structurally ordered material at long-range. On the other hand, the low detection limit imposed by the XRD technique does not allow estimating the existence or not of any trace of Ag phase less than 2%, if it exists in the form Ag nanoparticles grown on the surface of β - Ag_2MoO_4 microcrystals.¹⁶ The dipole moment (μ) for each polar solvent used in the syntheses is displayed in Table S1. Particularly, the decrease in μ values promoted a narrowing in the width of diffraction peaks and a change in Ag–O and Mo–O bond angles (Table S1 in Supporting Information).

The Rietveld method is based on the construction of diffraction patterns calculated according to a structural model.¹⁹ The calculated patterns are adjusted to fit the observed patterns and thus, provide the structural parameters of the material and diffraction profile. In our study, the Rietveld refinement was used to adjust the atomic positions, lattice parameters, and unit cell volume. All refinements were performed using the general structure analysis (GSAS) program.²⁰ Again, the structural refinements confirmed all β - Ag_2MoO_4 microcrystals have a spinel-type cubic structure without secondary phases (Fig. S1 and Table S2 in Supplementary Information).

Fig. 2 shows a schematic representation of a β - Ag_2MoO_4 structure modeled by means of Rietveld refinement data.

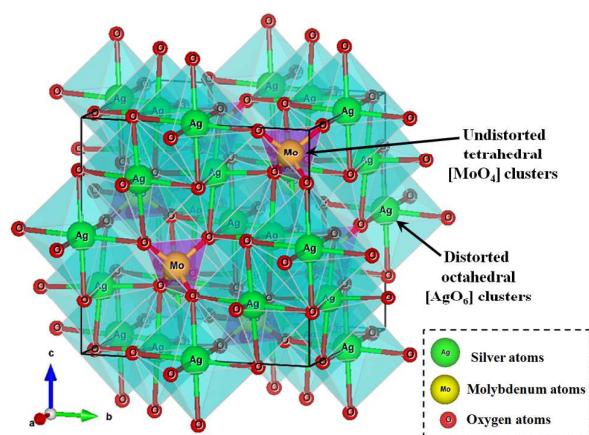
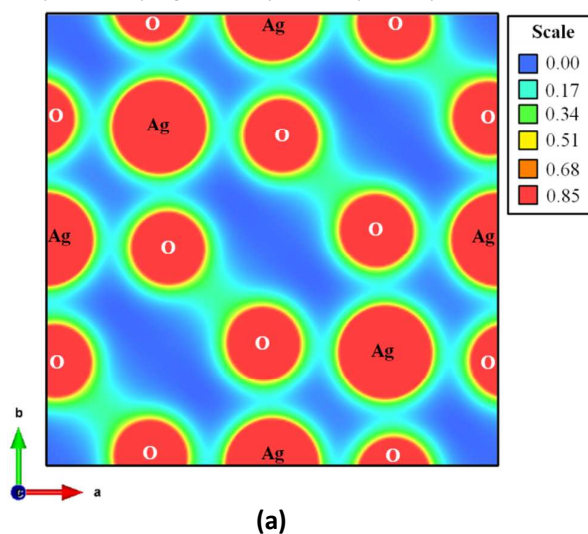


Fig. 2: Schematic representation of cubic β - Ag_2MoO_4 structure.

Lattice parameters and atomic positions estimated from Rietveld refinements were employed to model this structure by the Visualization for Electronic and Structural Analysis (VESTA) program (version 3.3.1 for Windows).²¹ The spinel-type cubic structure of β - Ag_2MoO_4 microcrystals is characterized by the space group ($Fd\bar{3}m$) with eight molecular formula per unit cell ($Z = 8$).¹⁵ In these structures, silver atoms are coordinated to six oxygens forming octahedral $[\text{AgO}_6]$ clusters. The molybdenum atoms are coordinated to four oxygens, which result in tetrahedral $[\text{MoO}_4]$ clusters. In principle, our Rietveld refinement data, especially the anisotropic displacement parameters (U) in Table S2 (Supplementary Information), indicate the existence of distorted octahedral $[\text{AgO}_6]$ clusters and undistorted tetrahedral $[\text{MoO}_4]$ clusters.

Fig. 3(a–c) shows the electron density models in (001), (010) and (110) planes for β - Ag_2MoO_4 crystals, respectively.



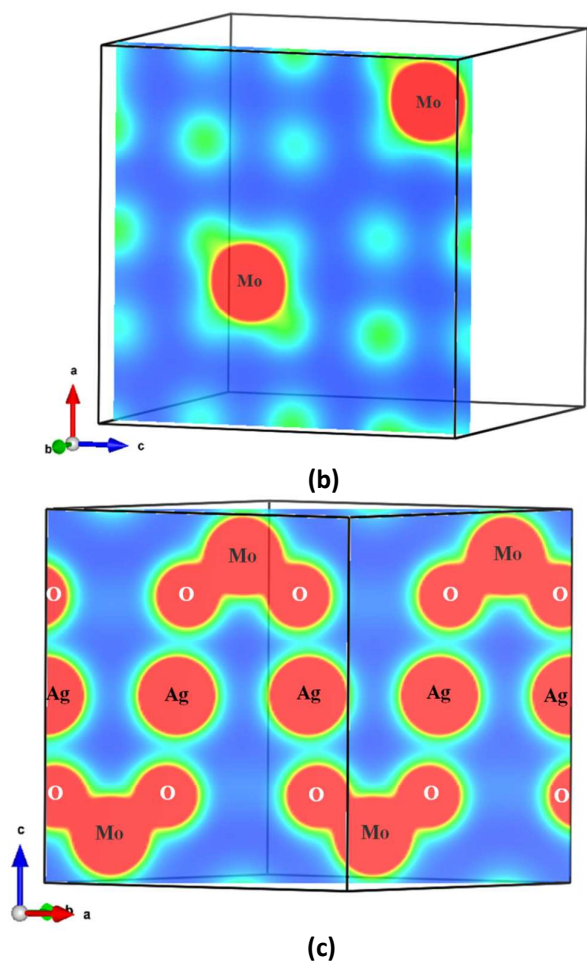


Fig. 3: Electron density maps on the (a) (001), (b) (010) and (c) ($1\bar{1}0$) planes of β - Ag_2MoO_4 microcrystals.

These electron density models were calculated by the Fourier transform of structure factors from structure parameters and atomic scattering factors of free atoms obtained from Rietveld refinement for β - Ag_2MoO_4 crystals at 60°C for 8 h, using H_2O as solvent. These data were used in VESTA program²¹ to model the electron density map. In these figures were displayed a color scale on each plane, which demonstrated zones with high and low electronic densities. In Fig. 3(a), the blue color regions are related to absence of electronic charge, while the red color areas exhibit a high electronic density. Moreover, it is possible to verify the four chemical Ag–O bonds located on a - and b -axis ($d_{x^2-y^2}$ orbitals) exhibits a slight atomic displacement, suggesting the existence of distortions (Fig. 3(a)). In (010) plane is found only two Mo atoms, the green area around the Mo atoms indicate the presence of four O atoms with short bond distance (Fig. 3(b)). Finally, ($1\bar{1}0$) plane revealed the Ag and Mo atoms are able to share a same oxygen, in which the bond distance between O–Ag–O is higher than O–Mo–O.

Fig. 4(a–e) shows the FE-SEM images and Fig. 4(f) illustrates the average crystal size of β - Ag_2MoO_4 microcrystals prepared with different polar solvents.

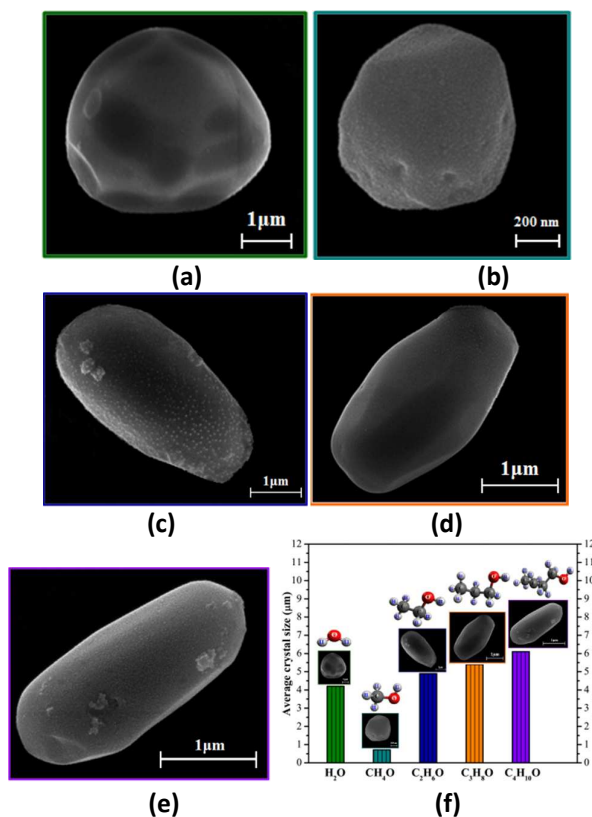


Fig. 4: FE-SEM micrographs of individual β - Ag_2MoO_4 microcrystals prepared with (a) H_2O , (b) CH_4O , (c) $\text{C}_2\text{H}_6\text{O}$, (d) $\text{C}_3\text{H}_8\text{O}$, (e) $\text{C}_4\text{H}_{10}\text{O}$, and (f) dependence of average crystal size in function of type of solvent.

In Figs. 4(a–e), the micrographs suggest a dependence of the crystal shape with the type of solvent. In principle, the increase in alcohol chains changes the crystal shape from irregular quasi-spherical (H_2O and CH_4O) to elongated crystals ($\text{C}_2\text{H}_6\text{O}$, $\text{C}_3\text{H}_8\text{O}$ and $\text{C}_4\text{H}_{10}\text{O}$). The smallest crystal size was noted for the samples prepared with CH_4O solvent (Fig. 4(b)), which can be related to its high-saturated vapor pressure. This solvent with low boiling point (64.7°C), when employed as a reaction media, promotes a weak interaction between the nuclei and favors the formation of small quasi-spherical β - Ag_2MoO_4 crystals.²² Some Ag nanoparticles grown on the surface of β - Ag_2MoO_4 microcrystals due to the accelerated electron beam from field-emission scanning electron microscope under high vacuum, phenomenon that has already been elucidated and discussed in previous papers.¹⁶ Another important information observed in these micrographs was an increase in average crystal size of β - Ag_2MoO_4 microcrystals with the decrease of solvent polarity (Figs. 4(f)). This result is in good agreement with FE-SEM images of β - Ag_2MoO_4 microcrystals illustrated in Fig. S2 (Supplementary Information). Therefore, the type of solvent is able to affect the morphological behavior of the system, especially, the formation and growth stages of primary nanoparticles. In addition, there is a growth preferential for the crystals formed with $\text{C}_2\text{H}_6\text{O}$, $\text{C}_3\text{H}_8\text{O}$ and $\text{C}_4\text{H}_{10}\text{O}$ solvents, as a type of template effect.

The optical band gap energy (E_{gap}) of β - Ag_2MoO_4 crystals was estimated by a modified Kubelka-Munk equation:^{23–25}

$$[F(R_{\infty})hv]^n = C_1(h\nu - E_{\text{gap}})^n \dots \dots \dots (1)$$

where, $F(R_{\infty})$ is the Kubelka-Munk function, R_{∞} is the reflectance ($R_{\infty} = R_{\text{sample}}/R_{\text{standard}}$; R_{standard} was magnesium oxide [MgO]), $h\nu$ is the photon energy, C_1 is a proportionality constant, E_{gap} is the optical band gap and n is a constant associated with different types of electronic transitions ($n = 0.5$ for a direct allowed, $n = 2$ for an indirect allowed, $n = 1.5$ for a direct forbidden and $n = 3$ for an indirect forbidden). For $\beta\text{-Ag}_2\text{MoO}_4$ microcrystals, the optical absorption spectra are governed by indirect electronic transitions.¹² In this typical physical phenomenon, after the electronic absorption process, electrons located in minimum energy states in the conduction band (CB) are able to go back for maximum energy states in the valence band (VB), but in distinct points in the Brillouin zone.²⁶ Based on this information, E_{gap} values of $\beta\text{-Ag}_2\text{MoO}_4$ microcrystals were calculated using $n = 2$ in Eq. 1.

Therefore, finding the $F(R_{\infty})$ value from Eq. 1 and plotting a graph of $[F(R_{\infty})hv]^2$ in function of $h\nu$, E_{gap} values were estimated for $\beta\text{-Ag}_2\text{MoO}_4$ microcrystals by extrapolating the linear portion of UV-vis curves.

Fig. 5(a–f) shows the UV-vis diffuse reflectance spectra and optical band gap (E_{gap}) values of $\beta\text{-Ag}_2\text{MoO}_4$ microcrystals synthesized in this study.

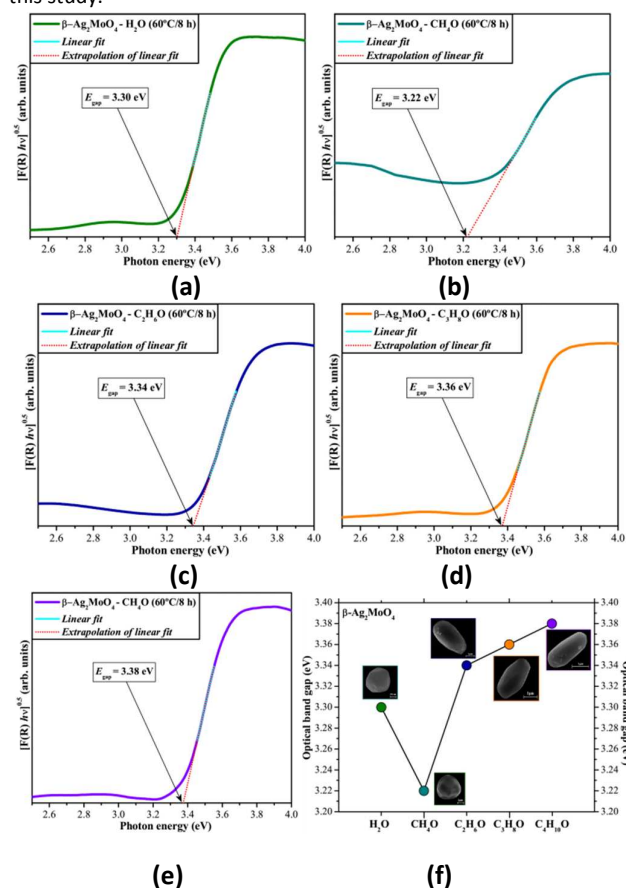


Fig. 5: UV-vis diffuse reflectance spectra of $\beta\text{-Ag}_2\text{MoO}_4$ microcrystals prepared with different polar solvents: (a) H_2O , (b) CH_4O , (c) $\text{C}_2\text{H}_6\text{O}$, (d) $\text{C}_3\text{H}_8\text{O}$, (e) $\text{C}_4\text{H}_{10}\text{O}$ and (f) evolution of optical band gap (E_{gap}) values of all microcrystals.

In Figs. 5(a–f), significant changes in E_{gap} values of $\beta\text{-Ag}_2\text{MoO}_4$ microcrystals were not verified, the only exception was the crystals formed with CH_4O solvent. Although the E_{gap} estimated by UV-vis measurements is considered qualitative, the calculated results imply that the microcrystals have distinct types and concentrations of structural and surface defects, such as oxygen vacancies, distortions on the O–Ag–O bonds, and porous surface. All defects are arising from the crystal formation and growth processes, which are influenced by the type of solvent used in the synthesis, as well as by the irreversible attachment (agglomeration) caused by the dynamics of particle-particle collisions. Consequently, these defects cause a symmetry break responsible for the lattice polarization, resulting in the presence of intermediary energy levels within the band gap.²⁷ Thus, the microcrystals synthesized with CH_4O (lower E_{gap}) have a lower density of intermediary energy states than the microcrystals prepared with other solvents.

In summary, monophasic $\beta\text{-Ag}_2\text{MoO}_4$ microcrystals were synthesized with different polar solvents (H_2O , CH_4O , $\text{C}_2\text{H}_6\text{O}$, $\text{C}_3\text{H}_8\text{O}$ and $\text{C}_4\text{H}_{10}\text{O}$) by a simple precipitation method at 60°C for 8 h. XRD patterns indicated all crystals are structurally ordered at long-range. Rietveld refinement data confirmed all microcrystals have a spinel-type cubic structure, which is composed of distorted octahedral $[\text{AgO}_6]$ clusters and undistorted tetrahedral $[\text{MoO}_4]$ clusters. The electron density models were employed to understand the polarization phenomenon and anisotropic atomic displacements in $[\text{O}–\text{Ag}–\text{O}]$ bonds. FEG-SEM images showed a dependence of formation and growth stages of these microcrystals with the type of polar solvent employed in the synthesis. The slight differences in E_{gap} values were caused by the existence of intermediary energy states within the band gap. These energetic states are originated by the defects, which differ in type and concentration between the microcrystals. We expect that this facile and controllable synthetic route can be used in the preparation of new complex metal oxides for future technological applications in solid-state lighting, solar cells, sensor, fuel cell and photocatalysis.

The Brazilian authors acknowledge the financial support of the Brazilian research financing institutions: CNPq (120482/2014-2; 350711/2012-7; 479644/2012-8), FAPESP (12/14004-5; 13/07296-2) and CAPES.

Notes and References

- 1 A.K. Arora, R. Nithya, S. Misra, T. Yagi, *J. Solid State Chem.* 2012, **196**, 391.
- 2 A. Beltrán, L. Gracia, E. Longo, J. Andrés, *J. Phys. Chem. C.* 2014, **118**, 3724.
- 3 C.H.B. Ng, W.Y. Fan, *Cryst. Growth. Des.* 2015, **15**, 3032.
- 4 D.P. Singh, B. Sirota, S. Talpatra, P. Kohli, C. Rebholz, S.M. Aouadi, *J. Nanopart. Res.* 2012, **14**, 781.
- 5 E.K. Fodjo, D.W. Li, N.P. Marius, T. Albert, Y.T. Long, *J. Mater. Chem. A.* 2013, **1**, 2558.
- 6 Z.Q. Li, X.T. Chen, Z.L. Xue, *Sci. China Chem.* 2013, **56**, 443.
- 7 E. Liu, Y. Gao, J. Jia, Y. Bai, *Tribol. Lett.* 2013, **50**, 313.
- 8 S.A. Suthanthiraraj, Y.D. Premchand, *Ionics.* 2004, **10**, 254.
- 9 F. Rocca, A. Kuzmin, P. Mustarelli, C. Tomasi, A. Magistris, *Solid State Ionics.* 1999, **121**, 189.

- 10 S. Brown, A. Marshall, P. Hirst, *Mater. Sci. Eng. A*. 1993, **173**, 23.
- 11 Y.V.B. De Santana, J.E.C. Gomes, L. Matos, G.H. Cruvinel, A. Perrin, C. Perrin, J. Andr es, J.A. Varela, E. Longo, *Nanomater. Nanotechnol.* 2014, **4**, 22.
- 12 A.F. Gouveia, J.C. Sczancoski, M.M. Ferrer, A.S. Lima, M.R.M.C. Santos, M.S. Li, R.S. Santos, E. Longo, L.S. Cavalcante, *Inorg. Chem.* 2014, **53**, 5589.
- 13 H. Jiang, J.K. Liu, J.D. Wang, Y. Lu, X.H. Yang, *CrystEngComm.* 2015, **17**, 5511.
- 14 S. Zhao, Z. Li, Z. Qu, N. Yan, W. Huang, W. Chen, H. Xu, *Fuel.* 2015, **158**, 891.
- 15 R.W.G. Wyckoff, *J. Am. Chem. Soc.* 1922, **44**, 1994.
- 16 J. Andr es, M.M. Ferrer, L. Gracia, A. Beltran, V.M. Longo, G.H. Cruvinel, R.L. Tranquilin, E. Longo, *Part. Part. Syst. Charact.* 2015, **32**, 646.
- 17 A. Patterson, *Phys. Rev.* 1939, **56**, 978.
- 18 G.K. Williamson, W.H. Hall, *Acta Metall.* 1953, **1**, 22.
- 19 H.M. Rietveld, *Acta Crystallogr.* 1967, **22**, 151.
- 20 A.C. Larson, R.B. Von Dreele, General structure analysis system (GSAS). Los Alamos: National Laboratory, 2001, pp. 124.
- 21 K. Momma, F. Izumi, *J. Appl. Crystallogr.* 2011, **44**, 1272.
- 22 K.G. Kanade, B.B. Kale, R.C. Aiyer, B.K. Das, *Mater. Res. Bull.* 2006, **41**, 590.
- 23 P. Kubelka, F. Munk, *Zeit. F ur. Tech. Physik.* 1931, **12**, 593.
- 24 A.E. Morales, E.S. Mora, U. Pal, *Rev. Mex. Fis. S.* 2007, **53**, 18.
- 25 R.A. Smith, *Semiconductors*, 2nd ed.; Cambridge University Press: London, 1978; p 434.
- 26 R. Lacombe-Perales, J. Ruiz-Fuertes, D. Errandonea, D. Mart nez-Garc a, A. Segura, *Eur. Phys. Lett.* 2008, **83**, 37002.
- 27 V.S. Marques, L.S. Cavalcante, J.C. Sczancoski, A.F.P. Alc ntara, M.O. Orlandi, E. Moraes, E. Longo, J.A. Varela, M.S. Li, M.R.M.C. Santos, *Cryst. Growth Des.* 2010, **10**, 4752.

GRAPHICAL ABSTRACT (CrystEngComm)

Rietveld refinement, morphology and optical properties of β - Ag_2MoO_4 microcrystals synthesized by a simple precipitation method using different polar solvents [water, methanol, ethanol, 1-propanol and 1-butanol]. The results indicated the β - Ag_2MoO_4 microcrystals with cubic structure are composed of distorted octahedral $[\text{AgO}_6]$ clusters and undistorted tetrahedral $[\text{MoO}_4]$ clusters.

